

NeutronOrch: Rethinking Sample-based GNN Training under CPU-GPU Heterogeneous Environments

Xin Ai, Qiange Wang, Chunyu Cao, Yanfeng Zhang, Chaoyi Chen, Hao Yuan, Yu Gu, Ge Yu

Northeastern University, China

{aixin0,wangqiange,chenchaoy,yuanhao}@stumail.neu.edu.cn,{zhangyf,guyu,yuge}@mail.neu.edu.cn

ABSTRACT

Graph Neural Networks (GNNs) have demonstrated outstanding performance in various applications. Existing frameworks utilize CPU-GPU heterogeneous environments to train GNN models and integrate mini-batch and sampling techniques to overcome the GPU memory limitation. In CPU-GPU heterogeneous environments, we can divide sample-based GNN training into three steps: sample, gather, and train. Existing GNN systems use different task orchestrating methods to employ each step on CPU or GPU. After extensive experiments and analysis, we find that existing task orchestrating methods fail to fully utilize the heterogeneous resources, limited by inefficient CPU processing or GPU resource contention.

In this paper, we propose NeutronOrch, a system for sample-based GNN training that incorporates a layer-based task orchestrating method and ensures balanced utilization of the CPU and GPU. NeutronOrch decouples the training process by layer and pushes down the training task of the bottom layer to the CPU. This significantly reduces the computational load and memory footprint of GPU training. To avoid inefficient CPU processing, NeutronOrch only offloads the training of frequently accessed vertices to the CPU and lets GPU reuse their embeddings with bounded staleness. Furthermore, NeutronOrch provides a fine-grained pipeline design for the layer-based task orchestrating method, fully overlapping different tasks on heterogeneous resources while strictly guaranteeing bounded staleness. The experimental results show that compared with the state-of-the-art GNN systems, NeutronOrch can achieve up to 4.61× performance speedup.

1 INTRODUCTION

Graph Neural Networks (GNNs) [46] are a novel class of Deep Neural Networks (DNNs) designed to process graph-structured data. They have demonstrated remarkable effectiveness across various applications, including social networks [23, 44, 51], neural machine translation [2], and recommender systems [7, 8]. GNNs aim to learn low-dimensional feature representations (i.e., embeddings) [13] for each vertex in a graph, enabling them to perform downstream graph-related tasks. Recently, GPUs have been extensively used to accelerate GNN training owing to their high memory bandwidth and massive parallelism [18, 22]. Machine learning systems like PyTorch Geometric (PyG) [9] and Deep Graph Library (DGL) [42] offer optimized GPU implementations and convenient programming interfaces, enhancing the training of GNNs on GPUs.

Considering the growing sizes of graphs in real-world applications, it becomes impractical to accommodate the entire graph and training data in the GPU memory [20, 27, 41]. As a result, the sample-based approach for training GNNs has emerged as a promising solution. This approach performs computations on sampled subgraphs, allowing the training of large input graphs with limited GPU resources [14, 50, 53]. In this approach, the input data,

including vertex features and graph structure, are stored in the host memory while the training process is offloaded to GPUs [42, 54]. The sample-based GNN training divides the training vertices into multiple batches, treating each batch as the smallest unit for training. To train on a batch, the training process first samples the K -hop subgraphs for the training vertices, following a given neighbor sampling rule. It then gathers the required vertex features based on the sampled subgraph and loads the subgraph and the involved vertex features onto the GPU. Finally, the GPU performs a forward and backward pass and updates the corresponding model parameters.

This computation mechanism, known as the **sample-gather-train** has gained widespread adoption in various popular GNN systems [25, 29–31, 37, 41, 42, 45, 47, 49]. These systems decouple the three steps and deploy them on computation devices to achieve high performance. Early systems [5, 25, 37, 41, 42] employ graph sampling and feature gathering on CPUs. These systems store the graph data in the CPU memory, perform CPU-based graph sampling, and collect the required features on the CPU side before transferring them to GPUs. This approach allows the GPUs to be dedicated solely to training tasks. On the other hand, some other systems [21, 29, 42, 45, 47, 49] leverage GPU-accelerated graph sampling. They store the graph topology in either GPU or pinned CPU memory and perform the sampling on GPUs, relieving CPUs from the heavy random memory access. Moreover, recent systems [25, 29, 45, 47, 49] also employ GPU-based feature gathering to optimize overall performance. They store the vertex feature completely or partially (with caching mechanism) on GPUs, converting the heavy host-GPU data communication and CPU memory access to efficient GPU global memory access. The GPU-based graph sampling and GPU-based feature caching can be used jointly to optimize performance.

Figure 1 overviews existing GNN systems and their task orchestrating methods using a 3-layer binary tree. Each path from the root to the leaf represents a specific task orchestrating method, where the CPU is selected when traversing the left child, and the GPU is selected when traversing the right child. Among the possible eight methods, since performing training on the CPU is not a wise option under CPU-GPU heterogeneous environments, the existing task orchestrating methods can be summarized into four categories.

Having conducted intensive experiments and analysis, we find that existing task orchestrating methods that decouple the computation based on the step do not fully utilize CPU-GPU heterogeneous resources. As many past works [21, 25, 29, 37, 49] have pointed out, CPU-based sampling and gathering steps are slow, leading to significant waiting time for the training step on GPUs to receive the input data. In contrast, Figure 1 illustrates that many systems [25, 29, 42, 45, 47, 49] rely on GPUs to handle two or three steps. Although GPU-based optimizations can enhance the performance of each step, there is a risk of GPU resource contention if many

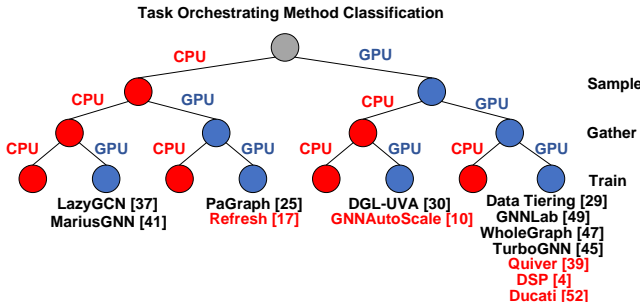


Figure 1: Classification tree of existing GNN systems and their task orchestrating methods.

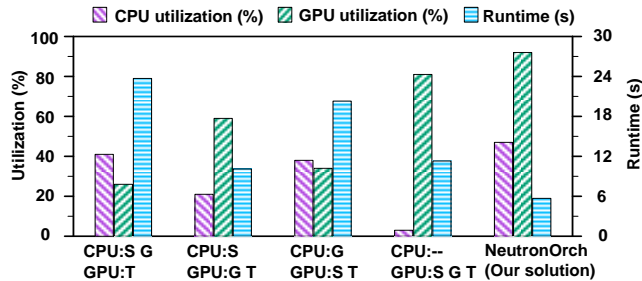


Figure 2: Comparison of resource utilization and per-epoch execution time for different task orchestrating methods. The S, G, and T represent the sample, gather, and train steps of sample-based GNN training.

steps are deployed on the GPU. This is because the training data, cached features, and graph topology need to be simultaneously stored within the constrained GPU memory while the computation kernels of sampling and training are completed for the limited GPU cores. To illustrate this, we run the four task orchestrating methods in DGL [42] and compare their performance in Figure 2. We evaluate the GPU utilization, CPU utilization, and per-epoch runtime for each method with a 3-layer GCN model on Reddit dataset. We can observe that the existing task orchestrating methods do not effectively utilize CPU-GPU heterogeneous resources. They either underutilize one side or fail to fully leverage the potential of both CPU and GPU, resulting in sub-optimal performance.

In this work, we rethink the roles of CPU and GPU in sampling-based GNN training and propose a hotness-aware layer-based task orchestrating method to optimize performance. Specifically, we observe that offloading the computation of the bottom layer to the CPU significantly reduces the computational load and memory footprint of GPU training. Therefore, unlike existing methods that allocate each step to a single device, we decouple the training task by layers and employ the computation of each sub-task (sample-gather-train) to a single device. In addition, the transfer volume between CPU and GPU can be reduced by aggregating and updating features into embeddings before the transfer begins.

Offloading the computation of a complete GNN layer to the CPU will make the CPU processing a new bottleneck if not carefully optimized. To address this issue, we propose a hotness-aware embedding caching method that reduces CPU computation by periodically computing the embeddings of frequently accessed vertices (i.e., hot vertices) and reusing them across batches. To sustain the correctness when training with reused embeddings, we extend

bounded staleness [6, 15, 31, 34] processing to guarantee that the reused embedding is within a given stale constraint.

Moreover, to further improve resource utilization, we propose a super-batch pipelined training that combines k adjacent batches into a super-batch and controls the update and reuse of hot embeddings among super-batches, overlapping GPU and CPU computation tasks while strictly guaranteeing bounded staleness.

By integrating the above techniques, we propose NeutronOrch, a sampling-based GNN system that can efficiently utilize the resources of heterogeneous CPU-GPU environments. We make the following contributions.

- We provide a comprehensive analysis of the resource underutilization problem associated with the task orchestrating methods in existing sample-based GNN systems.
- We propose a hotness-aware layer-based task orchestrating method that effectively leverages the computation and memory resources of the GPU-CPU heterogeneous system.
- We propose a super-batch pipelined training, which fully overlaps different tasks on heterogeneous resources while strictly guaranteeing bounded staleness.

We evaluate the performance of NeutronOrch using three popular GNN models, GCN [23], GraphSAGE [14], and GAT [40]. Experimental results demonstrate that, compared with five state-of-the-art GNN systems, DGL [42], Paragraph [25], GNNlab [49], DSP [4], and GNNAutoScale [10], NeutronOrch achieves up to 4.61 \times , 3.89 \times , 2.24 \times , 1.51 \times , and 4.34 \times speedups, respectively.

The rest of this work is summarized as follows. Section 2 presents the background information relevant to this work. Section 3 presents the experimental analysis of limitations related to existing task orchestrating methods. Section 4 provides a detailed description of the proposed optimization techniques, as well as the architecture and implementation of NeutronOrch. Section 5 analyzes the experimental results. Section 6 presents a discussion on related work. Section 7 concludes the paper.

2 BACKGROUND

We first briefly introduce Graph Neural Networks (GNNs) and the process of sample-based GNN training.

2.1 Graph Neural Networks

Graph-structured data serves as the input for Graph Neural Networks (GNNs), where each vertex or edge is associated with a high-dimensional feature vector. A typical GNN model consists of multiple layers that compute a low-dimensional embedding for each vertex. Each layer contains an aggregation phase and an update phase [55]. For example, in a GNN with L layers, during the aggregation phase of layer l , each vertex v combines its neighbors' embedding vectors at the $l-1$ layer with its own embedding vector to generate the aggregation result a_v^l using an aggregation function:

$$a_v^l = \text{AGGREGATE}(h_u^{l-1} | \forall u \in N_{in}(v) \cup \{v\}) \quad (1)$$

where $N_{in}(v)$ represents the incoming neighbors of vertex v , h_v^l represents the node embedding vector of vertex v at l -th layer, and h_v^0 is the input feature of vertex v . The aggregate functions can be sum, average, max/min, etc. Next, during the update phase, each vertex computes its output embedding vector h_v^l by applying an

Table 1: Notations

Notation	Description
a_v^l	aggregation results vector of vertex v at the l^{th} layer
h_v^l	embedding vector of vertex v at the l^{th} layer
A_i	Adjacency matrix of the i^{th} iteration
\hat{A}_i	Adjacency matrix after symmetric normalization of the i^{th} iteration
W_i^l	Weight matrix at the l^{th} layer of the i^{th} iteration
H_i^l	Embedding matrix at the l^{th} layer of the i^{th} iteration
Z_i^l	Input matrix to activation function at the l^{th} layer of the i^{th} iteration
$\nabla \mathcal{L}$	Gradient of the loss function
$\nabla_{Z_i^l} \mathcal{L} = \delta^l$	Gradient matrix of the loss \mathcal{L} with respect to Z_i^l at the l^{th} layer
$\nabla_{W_i^l} \mathcal{L}$	Gradient matrix of the loss \mathcal{L} with respect to W_i^l at the l^{th} layer
$g(W_i)$	Gradient of the loss function with respect to W at the i^{th} iteration
\mathcal{L}	Loss of the GNN
I	Number of iterations in an epoch or number of batches
L	Number of layers of GNN model
η	Learning rate
ϵ	Staleness bound

update function to the aggregation result a_v^l :

$$h_v^l = \text{UPDATE}(a_v^l, W_i^l) \quad (2)$$

After L layers, each vertex's feature vector becomes a low-dimensional embedding of its neighbors up to L hops away. These embeddings can be utilized for performing a wide range of tasks, such as node classification and link prediction.

In backpropagation, we first derive the recurrence to backpropagate the gradient. Let $\nabla_{h_v^{l-1}} \mathcal{L}$ denote the gradient of the loss \mathcal{L} with respect to $\nabla_{h_v^{l-1}}$. By the chain rule, the relation between $\nabla_{h_v^{l-1}} \mathcal{L}$ and $\nabla_{h_v^l} \mathcal{L}$ is:

$$\nabla_{h_v^{l-1}} \mathcal{L} = \frac{\partial \mathcal{L}}{\partial h_v^l} \frac{\partial h_v^l}{\partial a_v^l} \frac{\partial a_v^l}{\partial h_v^{l-1}} \quad (3)$$

The gradient $\nabla_{h_v^{l-1}} \mathcal{L}$ can be computed in two steps. First, compute the gradient of the aggregation result of vertex v . Then, compute the gradient $\nabla_{h_v^l} \mathcal{L}$ of vertex v .

$$\frac{\partial h_v^l}{\partial a_v^l} = \frac{\partial \mathcal{L}}{\partial h_v^l} \frac{\partial h_v^l}{\partial a_v^l} = \delta_v^l \text{UPDATE}' \quad (4)$$

$$\nabla_{h_v^{l-1}} \mathcal{L} = \text{AGGREGATE}'(a_u^l | \forall u \in N_{out}(v) \cup \{v\}) \quad (5)$$

where δ_v^l denotes $\nabla_{h_v^l} \mathcal{L}$. UPDATE' is the derivative of the activation function of UPDATE , and $\text{AGGREGATE}'$ is the derivative of the activation function of AGGREGATE . When all vertices compute the aggregated gradient, each vertex pulls the aggregated gradient of its outgoing neighbors and computes the gradient $\nabla_{h_v^{l-1}} \mathcal{L}$ according to $\text{AGGREGATE}'$.

2.2 Sample-based Mini-batch GNN Training

The aggregation and update phase of GNNs involves complex matrix and vector operations on large-scale graph data. GPUs are generally more suitable for handling such computational tasks. Machine learning systems like PyTorch Geometric (PyG) [9] and Deep Graph Library (DGL) [42] offer optimized GPU implementations and user-friendly programming interfaces, enhancing the training of GNNs on GPUs. A GNN model can be trained simply on GPUs by using whole-graph training [18, 22, 43], in which the whole graph is loaded into GPUs and each vertex aggregates its neighbor features. However, real-world graphs are often massive and include

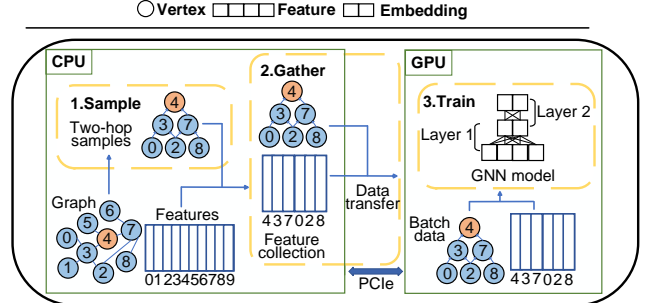


Figure 3: An example of sample-based GNN training for a two-layer GNN, where vertex 4 is the vertex with a ground-truth label for training.

Algorithm 1 Sample-based mini-batch GNN training (per epoch)

```

Input: graph structure  $G(V, E)$ , vertex features  $\{h_v^0 | v \in V\}$ , training set of vertices with ground-truth labels  $V_L$ , number of layers  $L$ , initial model parameters  $W_0^l$  for each layer  $l$ , and batch size  $b$ 
Output: updated parameters
1:  $\{V_0, \dots, V_I\} \leftarrow \text{split } V_L \text{ by batch size } b$ ; //split training vertices into  $I$  batches
2: for  $i = 1$  to  $I$  do
3:   /* Sample a subgraph for a batch of training vertices */
4:    $G_i \leftarrow \emptyset; V^F = V_i$ ;
5:   for  $l = L$  to  $1$  do
6:      $G^{l-1}(V^{l-1}, E^{l-1}) \leftarrow \text{sample}(V^F)$  // Sample one hop subgraph
7:      $G_i = G_i \cup G^{l-1}; V^F \leftarrow V^{l-1}$ 
8:   /* Gather the vertex features of sampled subgraph  $G_i$  */
9:    $H_i \leftarrow \{h_v^0 | v \in G_i\}$ 
10:  /* Train  $V_i$  with sampled subgraph  $G_i$  and update parameters */
11:  for  $l = 1$  to  $L$  do
12:    Forward compute the vertex embeddings with  $G_i, H_i, W_{i-1}^l$  based on Equation (1) and (2);
13:    Compute the loss  $\mathcal{L}$  and generate backward gradients;
14:    for  $l = L$  to  $1$  do
15:      Backward compute the gradients with  $G_i, H_i, W_{i-1}^l$  based on Equation (4) and (5);
16:      Update  $W_i^l$  based on  $W_{i-1}^l$  and  $\nabla W_{i-1}^l$ ;

```

high-dimensional vertex/edge features, which may exceed the memory capacity of GPUs [20, 27, 41]. To address the GPU memory limitation in training GNN models, state-of-the-art systems adopt sample-based mini-batch GNN training [25, 29, 37, 41, 42, 45, 47, 49].

The sample-based mini-batch GNN training splits the training vertices into multiple mini-batches. Each time it loads a batch of training vertices (with ground-truth labels) along with the sampled subgraph targeted at these vertices into GPUs for training [14, 50, 53]. Algorithm 1 elaborates the sample-based mini-batch GNN training process for a single epoch. It first splits training vertices V_L into I mini batches according to the batch size b (Line 1), then samples the multi-hop subgraph G_i of each batch (Line 3-9). The sampled subgraph is generated by a reverse traversal from the training vertices (Line 5-7). There is a fanout parameter to specify the number of sampled neighbors in the sample function per layer or per vertex for controlling the size of the sampled subgraph. It is noticeable that there exist other sampling schemes which help improve the accuracy, such as importance-aware sampling [5]. We show a simple and general case since the sampling scheme is not our focus in this paper. According to the sampled subgraph G_i , we launch the gathering step to collect the needed features H_i of sampled vertices (Line 9). The batch of training vertices V_i , the

gathered features H_i , and sampled subgraph G_i are then fed into the GNN model for training (Line 11-16). Specifically, there are a forward computation process of vertex embeddings (Line 11-12), loss computation with predicted labels and ground-truth vertex labels (Line 13), and a backward computation process of gradients (Line 14-15). The layer-wise parameters W^l are updated after each batch processing, so the parameters are updated multiple times instead of once in full-graph training.

Figure 3 shows an illustrative example of sample-based mini-batch GNN training model mapping to CPU-GPU heterogeneous execution environment. This is a 2-layer GNN model on a graph of 9 vertices with a training set containing only a single vertex 4. The input data, including graph data and high-dimensional features, are typically stored in host memory, while GPUs perform the GNN training on mini-batched and sampled subgraphs. In each training batch, this approach follows a **sample-gather-train** processing flow. Firstly, the graph sampling algorithm uniformly selects two neighboring vertices for each vertex. Secondly, the required vertex features are gathered based on the sampled subgraph and the training vertices. Then, they are loaded from the CPU to the GPU through a PCIe interconnect. Finally, the GPU performs forward and backward computations, computing and updating the model parameters correspondingly.

3 EXISTING SYSTEMS AND THEIR LIMITATIONS

A key challenge in achieving high-performance sample-based GNN training is orchestrating tasks on the GPU-CPU heterogeneous environments. Existing sample-based GNN systems [25, 29, 30, 37, 41, 42, 45, 47, 49] typically separate the training process based on the operations, i.e., **sample**, **gather**, and **train**, and assign each operation to the GPU or the CPU. However, they often exhibit suboptimal performance due to inefficient CPU processing or GPU resource contention. To illustrate this, we conduct a series of experiments to analyze the problems of existing task orchestration methods.

3.1 Existing Task Orchestrating Methods

In Figure 1, we classify task orchestrating methods and list representative systems. Among eight possible methods, CPU-based training is not utilized if a GPU is available on the platform. Therefore, we only consider placing sampling and gathering on different devices in the analysis. Further information regarding the used graphs, test platforms, and system configurations can be found in Section 5.

Case 1: Placing sampling and gathering on CPUs suffers from inefficient CPU processing We show an example of this case in Figure 4 (a). In this case, inefficient sampling and feature gathering on the CPU block the training pipeline, making data preparation the main bottleneck for overall performance.

Neighbor sampling traverses the graph to obtain a multi-hop sampled subgraph for each training vertex. It incurs massive computation and irregular memory access, which makes the limited computational resources of the CPU hard to accelerate [21]. On the other hand, deploying the gathering step on the CPU, including storing vertex features in the host memory and performing feature collection and transfer, also proves to be inefficient [25]. This inefficiency arises from two main factors. Firstly, the slot external PCIe

Table 2: The runtime breakdown (in seconds) of sample and gather steps on DGL with different datasets. The FC and FT represent the feature collection and feature transfer of the gather step. GNN: A 3-layer GCN [23].

Dataset	Sample	Gather (FC)	Gather (FT)	Total
Reddit	2.7/11%	9.1/38%	6.0/25%	23.7
Lj-large	128.8/14%	384.4/41%	252.5/27%	935.3
Orkut	78.8/10%	384.3/48%	249.1/31%	813.3
Wikipedia	209.4/12%	651.8/40%	570.9/33%	1669.1
Products	9.9/37%	7.2/27%	4.1/15%	26.8
Papers100M	11.5/32%	8.6/24%	6.4/18%	36.84

interconnect makes the host-GPU feature transfer much slower than GPU memory access [30]. Secondly, when loading the features of outermost neighbors, collecting and organizing the fragmented vertex feature into contiguous memory (to leverage the CUDA memory copy engine, cudaMemcpy) places a significant burden on CPU resources due to massive random memory access. We execute this task orchestrating method with a 3-layer GCN on all six real-world graphs and analyze the time distribution for sampling and gathering steps. As shown in Table 2, sampling and gathering steps occupy 19.3% and 61.2% of the total runtime, respectively. Specifically, the most significant overhead is the feature collection in the gathering step, which accounts for 36.3% of the total runtime.

On the other hand, the long sampling and gathering time also causes low GPU utilization. The training step in the GPU needs to wait for the slow CPU tasks. Figure 2 presents the average GPU utilization of the GCN trained on the Reddit dataset. We can observe that merely around 25% of the GPU computational resources are utilized when the CPU executes both sampling and gathering steps. Even if only separate sampling or gathering is performed on the CPU, the overall GPU utilization is still less than 65%.

Case 2: Placing sampling on the GPU suffers from GPU resource contention We show an example of this case in Figure 4 (b). In this case, the slow sampling can be accelerated through the massively parallel processing capability of GPUs. However, the sampling and training operations will compete for the GPU resources, leading to suboptimal overall performance.

Sampling-based GNN training typically employs a pipeline design that overlaps the different steps to achieve high performance in heterogeneous systems [25, 41, 42, 49]. Figure 5 (a) depicts an ideal pipeline implementation where the operations of three batches (numbered 1, 2, and 3) are fully overlapped. However, this optimization requires different steps to be executed on different resources. When placing sampling on the GPU, it competes for computation resources with the training step, leading to inefficient pipelining, as shown in Figure 5 (b). To illustrate this, we evaluate the performance of DGL with pipelined optimization and non-pipelined under both CPU-based and GPU-based sampling. We run a 3-layer GCN on the Reddit graph and report the results in Table 3. The GPU-based sampling with pipeline optimization reduces the runtime of its non-pipelined version by 43.1%, which is a lower improvement than the effect of pipeline optimization on CPU-based sampling. Furthermore, with pipeline optimization, GPU-based sampling shows inferior overall performance compared to CPU-based sampling.

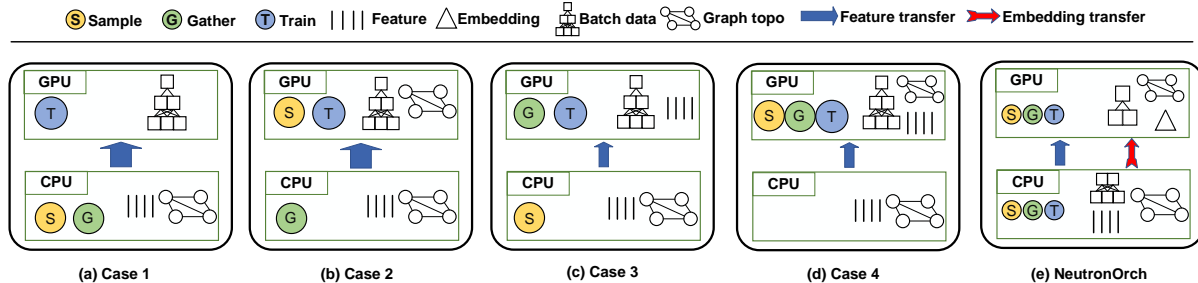


Figure 4: Illustration of the four task orchestrating methods and NeutronOrch. (a) Case 1 [37, 41]: Placing sampling and gathering on CPUs. (b) Case 2 [42]: Placing sampling on the GPU. (c) Case 3 [25]: Placing gathering on the GPU. (d) Case 4 [29, 45, 47, 49]: Placing sampling and gathering on the GPU. (e) Layer-based task orchestrating method of NeutronOrch. The width of the arrow is positively proportional to the transfer data volume. The volumes of the circles S, G, and T are proportional to the task amount.

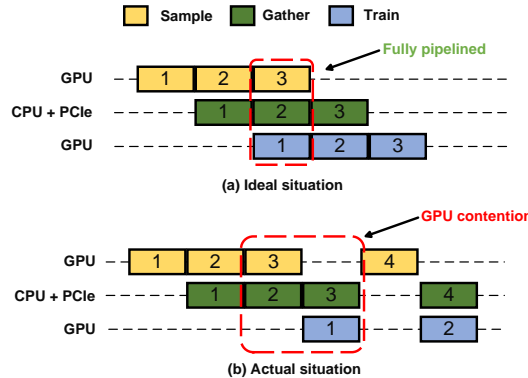


Figure 5: Two examples of multi-stream pipeline design in the ideal and actual situations.

Table 3: The runtime breakdown (in seconds) of a training epoch on DGL with CPU-based or GPU-based sampling. S, G, and T represent sample, gather, and train steps. GNN: A 3-Layer GCN [23]. Batch size 10000.

Configuration	S	G	T	Total	+pipeline
CPU-based sampling	2.28	2.84	2.76	7.88	3.42 (-56.6%)
GPU-based sampling	0.78	2.69	2.75	6.22	3.54 (-43.1%)

Case 3: Placing gathering on the GPU suffers from GPU memory contention GPU-based gathering method leverages GPU memory to cache the vertex features, converting the heavy host-GPU data communication to GPU memory access as much as possible [25, 29, 45, 47, 49]. However, the performance of GPU-based gathering method is influenced by the size of the configured memory buffer. We show an example of this case in Figure 4 (c). In actual training, a substantial amount of global memory must be allocated for storing the training data and intermediate results, leaving only a small portion of memory available for feature caching. If using a large cache buffer, the memory allocated for training has to be reduced, resulting in the training with a small batch size. Unfortunately, this trade-off may lead to inferior performance since the computational power of GPUs cannot be fully utilized [12, 19]. To illustrate the impact of batch sizes and cache ratios on performance, we conduct experiments on DGL using the 3-layer GCN model on the Wikipedia dataset. Figure 6 (a) and (b) display the results, demonstrating that training with a larger batch size is advantageous for GNNs in terms of achieving better GPU utilization. Although this consumes more GPU memory, it results in faster execution time for running an epoch.

Figure 6 (c) illustrates that a larger cache ratio contributes to a significant reduction in feature transfer volume during the gathering step. However, when using a batch size of 4096, we can only achieve a maximum cache ratio of about 0.05, leading to numerous cache misses. The maximum cache ratio is influenced by three factors: available GPU memory, total number of vertices, and feature dimensions. Therefore, the performance of cache policy will get worse when the graph topological data and feature dimensions increase, aligning with trends observed in GNN workloads [11, 14]. Due to GPU memory contention, the GPU cannot guarantee efficient acceleration of the gathering and training steps simultaneously.

Case 4: Placing sampling and gathering on the GPU suffers from GPU memory and resource contention We show an example of this case in Figure 4 (d). When all steps of sample-based GNN training are executed on the GPU, it results in GPU contention and CPU idle. The reasons for this situation have been discussed in cases 2 and 3. Firstly, the computation kernels of sampling and training compete for the limited GPU cores, leading to a slowdown in both. Secondly, the batch data for training and cache data for gathering contend with the limited GPU memory. When further making the GPU responsible for the sampling step, the GPU needs to additionally hold the graph topology data, which can make the GPU memory contention worse.

3.2 Summary

We conduct experimental analysis on different task orchestrating methods in GPU-CPU heterogeneous environments. Our observations reveal that step-based task orchestrating leads to an imbalanced allocation of computational and memory resources. Assigning two or more steps to the GPU may result in memory or GPU resource contention. On the other hand, assigning one or two steps to the CPU may cause inefficient CPU processing becomes a bottleneck. A well-designed CPU-GPU heterogeneous system should ensure adequate and balanced CPU and GPU utilization to achieve optimal performance. However, the step-based task orchestrating methods fail to achieve this. This motivates us to design a resource-balanced task orchestrating method.

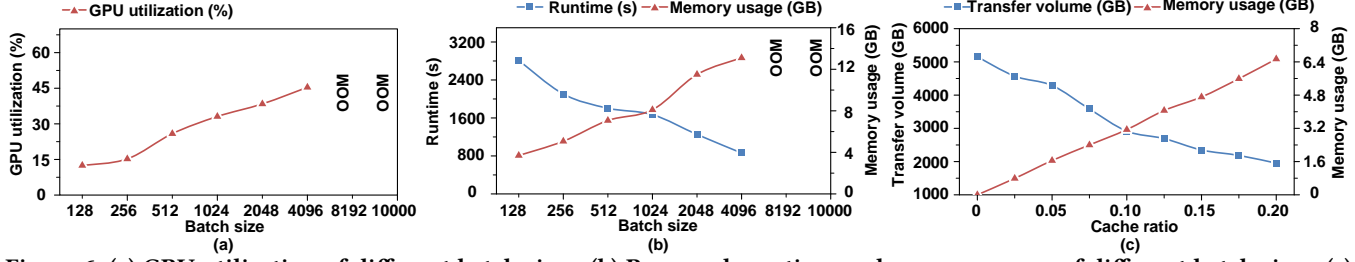


Figure 6: (a) GPU utilization of different batch sizes. (b) Per-epoch runtime and memory usage of different batch sizes. (c) Transfer volume and memory usage of different cache ratios.

4 NEUTRONORCH

4.1 System Overview

We propose NeutronOrch, a sample-based GNN training system that effectively improves CPU and GPU resource utilization through two critical techniques.

Hotness-aware layer-based task Orchestrating. Unlike step-based task orchestrating methods, NeutronOrch eliminates the constraint of placing the entire step on the CPU or GPU. Our approach decouples the training process by layer and employs the computation of each sub-task (sample-gather-train) to a single device. On the other hand, to prevent the CPU computation from becoming a bottleneck, we control the CPU to only compute the embeddings for the hot vertices that are frequently accessed while enabling the GPU to reuse these embeddings across batches within bounded staleness.

Super-batch pipelined training. Concurrently executing sub-tasks deployed on the GPU and CPU is essential to achieve high performance. However, it is challenging in NeutronOrch because the layer-based task orchestrating creates cross-layer data dependencies between the CPU and GPU training process. To solve this, we propose a super-batch pipelined training. In each super-batch, the CPU and GPU execute sub-tasks concurrently and independently of each other so that the training process is fully pipelined. In addition, this pipeline design also ensures that historical embeddings from the previous super-batch are only utilized within the current super-batch, enabling strict bounded staleness.

4.2 Hotness-Aware Layer-based Task Orchestrating

In this section, we give a detailed discussion on the hotness-aware layer-based task orchestrating. It maximizes CPU-GPU resource utilization based on two principles. Firstly, partitioning the tasks in a fine-grained manner and balancing the workload on CPU and GPU. Secondly, reducing the interaction between CPU and GPU to minimize communication overhead.

4.2.1 Layer-based Task Orchestrating. We find that the training process of sample-based GNN training can be divided not only by step but also by the GNN layer. As shown in Figure 4 (e), the CPU is responsible for the bottom layer computation of GNN training, while the GPU is responsible for the computation of the other layers. The CPU exhibits an inherent advantage when executing the bottom layer. Firstly, as the storage of features, the CPU can directly perform the GNN computation of the bottom layer without executing the time-consuming feature collection stage. Secondly, the data transfer volume between the CPU and GPU will decrease

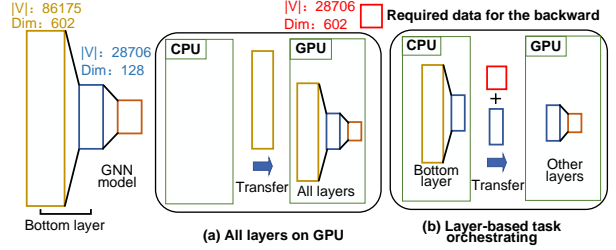


Figure 7: Workload and transfer volume of all layers on GPU and the layer-based task orchestrating, where $|V|$ represents the number of vertices and Dim represents the dimension of features or embeddings. GNN: A 2-Layer GCN [23]. Dataset: Reddit.

as the transfer objects are changed from the neighbors' features to the computed embeddings.

In this layer-based task orchestrating method, an additional data transfer stage is required in the backward pass for transferring the gradient back to the bottom layer in the CPU. To improve training efficiency, we move the backward computation of the bottom layer to GPU. Specifically, the required data for the gradient computation is transferred to the GPU along with the computed embeddings in the forward computation. Take the GCN [23] algorithm as an example. The aggregated neighbor representation and newly computed vertex embedding are transferred to the GPU.

We execute a two-layer GCN on the Reddit dataset to evaluate the impact of the layer-based task orchestrating method on the workload and transfer volume in the training process. The training batch size is 10000, and four random neighbors are sampled for a vertex in each layer. We count the number of vertices and the feature or embedding dimension of each model layer. As shown in Figure 7, the number of vertices in the outermost layer is three times that in the middle layer (86175 vs. 28706), positively related to the number of sampled neighbors (i.e., fanout). Meanwhile, the embedding dimension of the middle layer is generally smaller than the features in the outermost layer. Thus, despite introducing additional transmission for backward computation on the GPU, the layer-based task orchestrating method still has a smaller transfer volume. On the other hand, this method enables more GPU memory available for training data. Because we don't need to cache vertex features, the vertex features are aggregated and updated on the CPU. In addition, the CPU and GPU jointly maintain the training data in the train step, resulting in reduced GPU memory usage for the same batch size. By employing this layer-based task orchestrating method, we significantly reduce the computational load and memory footprint of GPU training.

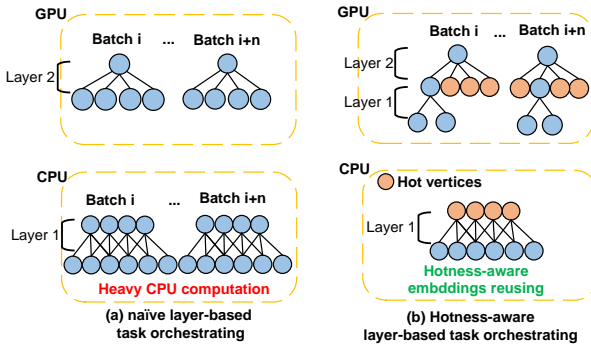


Figure 8: An illustrative of CPU and GPU workload in naive layer-based task orchestrating and hotness-aware layer-based task orchestrating.

4.2.2 Hotness-aware Embedding Reusing. As shown in Figure 8, executing a complete bottom layer in the CPU does not guarantee that it will not become a new bottleneck. The layer-based task orchestrating method must address the issue of inefficient CPU processing. Previous studies on cache policies have demonstrated that a subset of vertices is frequently accessed during sample-based GNN training [25, 29, 49]. The frequently accessed vertex is commonly referred to as the "hot vertex." By caching the features of these vertices in the GPU, existing works can avoid repeatedly loading them from the host memory. Similarly, by only computing hot vertices embeddings in the CPU and allowing the GPU to reuse these embeddings between batches within bounded staleness [6, 15, 34], our task orchestrating method can substantially decrease the computational load on the CPU.

The main idea of reusing embeddings within bounded staleness is to maintain the historical embedding $\tilde{h}_i^{(l)}$ for exact embedding $h_i^{(l)}$ as an affordable approximation with a given bound [6, 15, 34]. Bounded staleness expects $\tilde{h}_i^{(l)}$ and $h_i^{(l)}$ to be similar if the model weights do not change too fast during the training. In NeutronOrch, we use the number of model parameter updates, i.e., the number of batches, as the bound. Specifically, if the bound is N , a recently computed embedding can be reused within the subsequent N batches. Using historical embeddings avoids the need for aggregating neighbor features and the associated backward propagation. This not only reduces the amount of raw features to load but also minimizes the CPU workload. We will provide the theoretical analysis of the convergence guarantee for NeutronOrch in Section 4.3.2.

Following this idea, the CPU should handle the training of the bottom layer limited to the hot vertices. This allows for a higher reuse probability with minimal CPU load. Before the training begins, similar to the caching policy, NeutronOrch requires a preprocessing stage to prepare the hot vertices queue. We employ the Pre-Sample method [49] for each training vertex to sample it multiple times, recording the sampled frequencies (i.e., hotness) of the bottom layer vertices. Then, we determine the hot vertices queue based on their hotness and hot vertices ratio.

Figure 8 illustrates an example of the hotness-aware layer-based task orchestrating method. During the training, for hot vertices, the CPU samples them in one hop and computes the embeddings for them. The GPU pulls the hot vertices embeddings from the CPU

in each batch on demand. For the non-hot vertices in the bottom layer, the GPU will pull the features of their sampled vertices. To reduce the computation in the CPU, the GPU reuses the hot vertices embeddings with bounded staleness. To maintain model accuracy, it is crucial to ensure that all versions (batch number) of the hot vertices embeddings remain within a specified bound [6, 15, 31, 34]. We ensure that the embedding of all hot vertices is recomputed at least once in each epoch referring to VR-GCN [6] so that the staleness of the historical embeddings is bounded. By employing this method, we effectively reduce the computation volume in the CPU, mitigating the risk of CPU computation becoming a bottleneck.

4.3 Super-batch Pipelined Training

The complete overlap of tasks across diverse resources is essential to achieve high performance in heterogeneous systems. However, it is challenging in NeutronOrch because the layer-based task orchestrating creates cross-layer data dependencies between the CPU and GPU training process. Figure 9 (a) illustrates this situation in NeutronOrch, which sets stale bound to one epoch. The CPU updates the hot vertices embeddings when it reaches the bound, and the training on GPU must wait for the CPU to complete all the hot vertices embeddings update. Consequently, the pipelined execution of CPU and GPU computations is hindered, resulting in inefficiencies and resource wastage.

This section presents a comprehensive exploration of the super-batch pipeline design, starting with an overview, followed by a detailed examination of each stage. More importantly, we discuss the data dependencies resulting from the interleaving of CPU and GPU computations and propose strategies to manage it effectively.

4.3.1 Pipeline Design. During sample-based GNN training, each epoch contains many batches. As shown in Figure 9 (a), it is time-consuming for the CPU to compute hot vertices embeddings for all batches in an epoch and make GPU idle. In addition, the model weights are updated after one batch finishes. As a result, the hot vertices embeddings may be too stale for batches that start training later. To address these two issues, we reduce the stale bound from one epoch to multiple batches. Firstly, the hot vertices embeddings update in the CPU is partitioned into multiple sub-computing tasks, each of which computes the hot vertices embeddings for subsequent multiple batches, which provides more opportunities for pipelined designs. Secondly, more tightly controlled bounded staleness can help ensure model accuracy.

Before training starts, NeutronOrch combines n batches into a single super-batch. Then, we select a hot vertices queue for each super-batch. As shown in Figure 9, this is an illustrative example of a super-batch pipelined training when $n = 4$. During the pipelined training, the CPU computes the bottom layer embeddings of hot vertices for the next super-batch. In each super-batch, the GPU computes n batches of training for a given batch size, sharing the historical embeddings provided by the CPU from the last super-batch. The super-batch pipeline has a shorter CPU embedding update period than selecting hot vertices from all training vertices, effectively maintaining bounded staleness. Our pipeline design consists of four stages, each serving a specific purpose. We now elaborate on these individual stages.

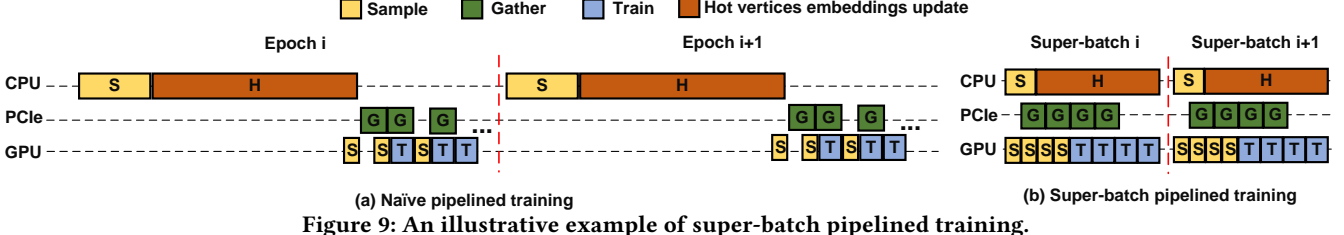


Figure 9: An illustrative example of super-batch pipelined training.

Stage 1: Sampling. The sampling tasks are divided between the CPU and GPU. Firstly, the CPU samples the hot vertices in one hop and generates a subgraph for bottom-layer training. Next, the GPU initiates n -hop sampling, and upon reaching the bottom layer, it skips the vertices previously sampled by the CPU and incorporates the CPU’s sampling outcomes. Meanwhile, the GPU completes n rounds of sampling before n training rounds to mitigate potential resource contention between the sampling and training kernels.

Stage 2: Hot vertices embeddings update on CPU. The CPU is responsible for updating the embeddings of the hot vertices intended for the subsequent super-batch within each super-batch. Once the CPU completes the sampling of hot vertices for the next super-batch, it promptly performs aggregation and updates on these vertices to obtain embeddings. The CPU conducts training based on the hotness order of the vertices and utilizes the most recent version of parameters supplied by the GPU.

Stage 3: Gathering. During the gathering step, the historical embeddings of hot vertices and the non-hot vertices’ features are transferred. After being transferred, the historical embeddings of the hot vertices will be cached in the GPU for use in other batches within the super-batch.

Stage 4: Training on GPU. The GPU training starts after n rounds of GPU sampling. During the forward pass, the GPU pulls the historical embeddings of hot vertices in the bottom layer from either the CPU or the GPU cache. For other layers, the GPU performs aggregation and updates alternately as normal.

Bounded Staleness. The CPU trains hot vertices in order of hotness and utilizes the latest model parameters. Therefore, the versions (batch number) of the model parameters vary within a hot vertices queue. As shown in Figure 9 (b), during the first super-batch, the hot vertices in the CPU may have versions ranging from 0 to $n-1$. In the second super-batch, when the GPU pulls hot vertices embeddings from the CPU, it may receive historical embeddings with model parameters that are older than the current version.

To minimize staleness, the CPU must complete the hot vertices embeddings update for the next super-batch within a single super-batch. This limitation ensures that the version gap remains within two super-batch, effectively preventing excessive staleness. Figure 9 (b) illustrates that the most significant version gap may occur in the last batch of the second super-batch. During this batch, the model parameter version is $2n-1$, and it may utilize historical embeddings from the previous super-batch with a model parameter version of 0. For the other batches, most embeddings experience staleness smaller than the upper bound of $2n-1$, with a version gap ranging from 1 to $2n-1$. If the CPU fails to complete the embeddings update before the GPU completes training the last batch in a super-batch, the hot vertices ratio will be decreased. Conversely, the CPU will raise the hot vertices ratio, maximizing the utilization.

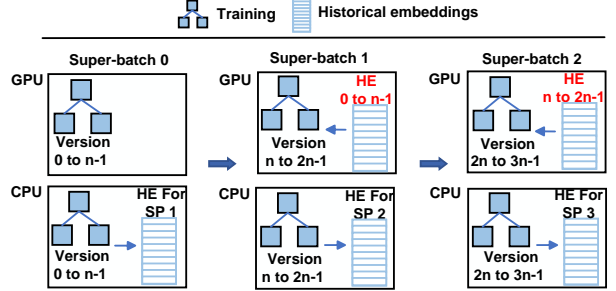


Figure 10: An example of the NeutronOrch’s buffer management policy. n represents the model parameter version, and HE represents the historical embedding.

4.3.2 Buffer management. To prevent resource contention with training processing, it is necessary to design the GPU memory allocation for caching the hot vertices embeddings. As implemented in the super-batch pipelined training, the GPU retrieves the historical embeddings from the CPU as needed and caches them for reusing. The cached data of hot vertices can be managed by maintaining a shared memory space in the GPU and a pinned memory space in the CPU. As depicted in Figure 10, within each super-batch, the GPU replaces the outdated embeddings with the embeddings provided by the previous super-batch. It is necessary to estimate the maximum GPU memory allocation for this space. Considering the batch size and the sample fanout, we can compute the maximum number of vertices in the bottom layer, denoted as V_{\max} . Subsequently, the maximum number of bottom layer vertices for a super-batch can be determined as $n \times V_{\max}$. Therefore, determining the appropriate GPU memory allocation for the shared memory space depends on the hot vertices rate ranging from 0 to 1 and $k \times V_{\max}$.

4.4 Convergence Analysis

In this section, we provide a theoretical analysis of convergence guarantee for NeutronOrch. Bounded staleness has been widely used by machine learning systems [6, 15, 31, 34, 49], and we present the theoretical analysis referring to the SANCUS [34] and VR-GCN [6]. To ensure bounded staleness, NeutronOrch designs super-batch pipelined training to limit the version (batch number) bound to $2n$, where n is the number of batches in a super-batch. In this process, we monitor the model weight variation between adjacent super-batches, and the maximum model weight variation ϵ that can be tolerated be defined as $\epsilon = \max \Delta \|W\| \times 2n$, where $\max \Delta \|W\|$ denotes the maximum value variation of W in a model weight update. With this staleness bound, we deduce the convergence guarantee as follows.

- **Proposition 1** provides the necessary and fundamental inequality operations required for the theoretical analysis;

- **Lemma 1** states that by imposing bounded staleness on the weights, the approximations of the embeddings and intermediate matrix results are close to the exact results;
- **Lemma 2** further demonstrates that the approximations of gradients in the training process closely match the exact gradients;
- **Theorem 1** concludes that the weight changes during training occur at a sufficiently slow rate, ensuring that the gradients are asymptotically unbiased and guaranteeing convergence;

Proposition 1. Let $\|A\|_\infty = \max_{ij} |A_{ij}|$, then we have:

$$\begin{aligned}\|AB\|_\infty &\leq \text{col}(A) \|A\|_\infty \|B\|_\infty \\ \|A \odot B\|_\infty &\leq \|A\|_\infty \|B\|_\infty \\ \|A + B\|_\infty &\leq \|A\|_\infty + \|B\|_\infty\end{aligned}$$

where, $\text{col}(A)$ denotes the number of columns of the matrix A , \odot denotes the element wise product.

This proposition has been proved by VR-GCN [6], and we omit the proof. We further denote C as the maximum number of columns that exist in our analysis.

Lemma 1, lemma 2, and Theorem 1 have also been proved by SANCUS [34] and VR-GCN [6], and we omit the proof and give the necessary and sufficient conditions for their establishment.

lemma 1. Assume all the activations are ρ -Lipschitz, the $\|W_i\|_\infty$ and $\|\hat{A}_i\|_\infty$ are bounded by some constant B , and the historical weights \tilde{W}_i are close to the exact weights W_i with the staleness bound ϵ where $\|\tilde{W}_i - W_i\| \leq \epsilon, \forall i$. Then the approximation error of the stale embedding \tilde{H} and stale activation \tilde{Z} is bounded by some constant K that depends on ρ, C, B : $\|H_i^l - \tilde{H}_i^l\|_\infty < \epsilon K, \forall i > I, l = 1, \dots, L - 1$; $\|Z_i^l - \tilde{Z}_i^l\|_\infty < \epsilon K, \forall i > I, l = 1, \dots, L$.

lemma 2. Assume that activation function $\sigma(\cdot)$ and the gradient $\nabla \mathcal{L}$ are ρ -Lipschitz, the $\|\nabla \mathcal{L}\|_\infty, \|\hat{A}_i\|_\infty, \|W_i\|_\infty$, and $\|\sigma'(Z_i)\|_\infty$ are bounded by some constant B , and the historical weights \tilde{W}_i are close to the exact weights W_i with the staleness bound ϵ where $\|\tilde{W}_i - W_i\| \leq \epsilon, \forall i$. Then the approximation error of the gradient $\tilde{g}(W_i)$ is bounded by some contents: $\|\mathbb{E}\tilde{g}(W_i) - \nabla \mathcal{L}(W_i)\|_\infty \leq \epsilon K$ and $\forall i > I$, where K depends on ρ, C, B .

Theorem 1. Given the local minimizer W^* . Assume that (1) the activation $\sigma(\cdot)$ is ρ -Lipschitz, (2) the gradient of the loss function $\nabla \mathcal{L}(W_i)$ is ρ -Lipschitz and bounded, (3) The gradient matrices $\|\tilde{g}(W)\|_\infty, \|g(W)\|_\infty$ and $\|\nabla \mathcal{L}(W)\|_\infty$ are bounded by some constant $G > 0$. (4) The loss $\mathcal{L}(W)$ is ρ -smooth, i.e.,

$$|\mathcal{L}(W_2) - \mathcal{L}(W_1) - \langle \nabla \mathcal{L}(W_1), W_2 - W_1 \rangle| \leq \frac{\rho}{2} \|W_2 - W_1\|_F^2, \forall W_1, W_2$$

, where $\langle A, B \rangle = \text{tr}(A^T B)$ is the inner product of matrix A and matrix B . Then, there exists $K > 0$, s.t., $\forall N > I$, if we run SGD for $R \leq N$ iterations, where R is chosen uniformly from $[I + 1, \dots, N]$ and the learning rate $\eta = \min\{\frac{1}{\rho}, \frac{1}{\sqrt{N}}\}$, we have:

$$\mathbb{E}_R \|\nabla \mathcal{L}(W_R)\|_F^2 \leq 2 \frac{\mathcal{L}(W_1) - \mathcal{L}(W^*) + \frac{\rho K}{2}}{\sqrt{N}}$$

when $N \rightarrow \infty$, $\mathbb{E}_R \|\nabla \mathcal{L}(W_R)\|_F^2 \rightarrow 0$, the above concludes that the convergence is guaranteed.

Table 4: Dataset description.

Dataset	V	E	ftr. dim	#L	hid. dim
Reddit [14]	232.96K	114.61M	602	41	256
Lj-large [1]	10.69M	224.61M	400	60	256
Orkut [48]	3.1M	117M	600	20	160
Wikipedia [24]	13.6M	437.2M	600	16	128
Products (PR) [16]	2.4M	61.9M	100	47	64
Papers100M (PA) [16]	111M	1.6B	128	172	64

Table 5: The competitor systems.

System	Sample	Gather	Train
DGL [42]	CPU	CPU	GPU
PaGraph [25]	CPU	GPU	GPU
GNNLab [49]	GPU	GPU	GPU
DGL-UVA [30]	GPU	CPU	GPU
GAS [10]	GPU	CPU	GPU
DSP [4]	GPU	GPU	GPU
NeutronOrch (ours)	CPU-GPU	CPU-GPU	CPU-GPU

5 EVALUATION

We implement NeutronOrch based on NeutronStar [43] and LibTorch (v1.9) [33]. This section evaluates the performance of NeutronOrch using representative GNN models and real-world datasets.

5.1 Experimental Setup

Environments. Single GPU experiments are conducted on an Aliyun server equipped with an Intel Xeon Platinum 8163 CPU (48 cores and 368 GB main memory) and NVIDIA V100 (16GB) GPU. The multi-GPU experiments are conducted on an Aliyun server equipped with an Intel Xeon Platinum 8163 CPU (96 cores and 736 GB main memory) and eight NVIDIA V100 (16GB) GPUs. The eight GPUs are connected to the CPU via four PCIe-3.0 switches and equipped with NVLink interconnects similar to NVIDIA DGX-1 [32]. The GPU is enabled with CUDA 11.4 runtime and 418.67 drivers, and the host side is running Ubuntu 18.04 with Linux kernel version 4.13.0. All the source codes are compiled with O3 optimization.

GNNs and model configurations. We evaluate NeutronOrch using three representative GNN models: GCN [23], GraphSAGE [14], and GAT [40]. The training batch size is set to 1024 by default. In the comparison with other systems, the model depth is set to 3, and the sampling fan-out is set to [25, 10, 5]. When using more layers for performance evaluation, sampling fan-out beyond 3 layers will be set to 5, i.e., [25, 10, 5, 5 ...].

Datasets. For evaluation, we utilize six real-world graph datasets, as listed in Table 4. These include Reddit [14] and Orkut [48], which are social networks, the Wikipedia (Wiki) network [24] comprising wikilinks from the English Wikipedia, the LiveJournal communication network (Lj-large) [1]. The Products (PR) [16] dataset is based on Amazon's co-purchasing network. The Papers100M (PA) [16] is a citation graph, where each vertex represents a paper and the edge represents the citation relation. The "ftr. dim" column represents the dimension of vertex features, the "#L" column represents the number of vertex classes, and the "hid. dim" column represents the embedding dimension of the hidden layer output. For graphs without ground-truth properties (Lj-large, Orkut, and Wikipedia), we use randomly generated features, labels, training (65%), test (10%), and validation (25%) set division.

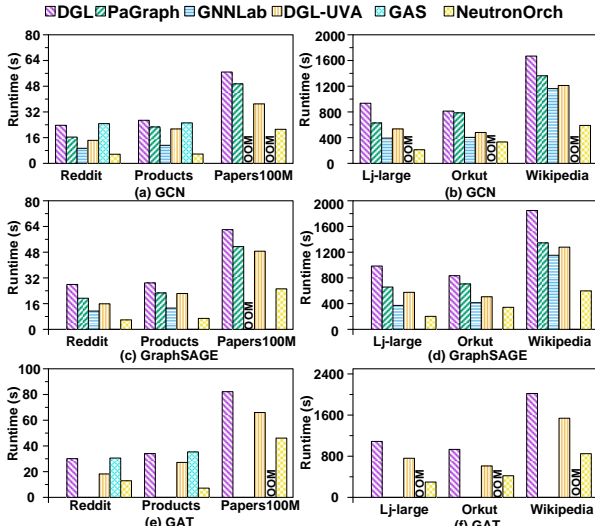


Figure 11: Overall training performance comparison (“OOM” denotes out of memory).

Baselines. We compare NeutronOrch with DGL [42], DGL-UVA [30], PaGraph [25], GNNLab [49], GNNAutoScale (GAS) [10], and DSP [4]. All comparison systems use GPUs to conduct training. DGL and DGL-UVA store both the graph structure and features in CPU memory. The difference is that DGL conducts sampling using the CPU, while DGL-UVA conducts sampling using the GPU by utilizing the UVA technique. PaGraph and GNNLab utilize GPU-based feature caching to reduce CPU-GPU communication. PaGraph conducts the sampling using the CPU, and GNNLab stores the graph structure in GPU memory and conducts the sampling using the GPU. GAS conducts feature gathering in the CPU, and it utilizes historical embedding to accelerate training. However, GAS does not provide bounded staleness, and historical embeddings are reused among an epoch. DSP is a multi-GPU GNN training system that uses multi-GPU cooperative sampling. It also caches the graph topology and popular vertex features in GPU memory to accelerate the gathering step. All these systems use the four specific step-based task orchestrating methods as discussed in Section 3. In the single GPU experiments, we compare NeutronOrch with five systems: DGL [42], DGL-UVA [30], PaGraph [25], GNNLab [49], and GAS [10]. In multi-GPU experiments, we compare NeutronOrch with four systems: PaGraph [25], DGL-UVA [30], GNNLab [49], and DSP [4]. We present the details of the compared systems in Table 5.

5.2 Single GPU Performance

Figure 11 shows the end-to-end training time of one training epoch for all GNN systems. Note that GNNLab [49] and PaGraph [25] do not provide GAT support, and GAS [10] does not provide GraphSAGE support.

(1) Comparison with DGL [42]: NeutronOrch achieves a speed-up ranging from $2.36\times$ (for GAT on Reddit) to $4.91\times$ (for GAT on PR) compared to DGL. DGL exhibits inferior performance compared to the other systems due to inefficient CPU-based sampling and gathering steps. As discussed in Section 3, DGL’s task orchestrating method requires the CPU to perform both the sampling step and feature collection in the gathering step. The computational

resources of the CPU are insufficient for effectively accelerating the sampling step in parallel, and they are also unable to handle the frequent random memory access required for feature collection. These two steps account for a substantial portion of the total runtime, resulting in considerable waiting time for the GPU. NeutronOrch effectively avoids inefficient CPU processing by selectively computing historical embeddings for hot vertices on the CPU. Hot vertices typically account for only a fraction of all training vertices, and historical embeddings can be reused multiple times across multiple batches, effectively reducing computation on the CPU.

(2) Comparison with PaGraph [25]: NeutronOrch achieves a speed-up ranging from $2.04\times$ (for GraphSAGE on PA) to $3.89\times$ (for GCN on PR) compared to PaGraph. PaGraph uses GPU-based gathering, reserving a portion of GPU memory for caching the features of high-degree vertices. The performance of PaGraph is limited by inefficient CPU sampling and GPU memory contention. As discussed in Section 3, the hit ratio of cache policy decreases as the feature dimension and batch size increase due to the limited GPU memory. By employing the hotness-aware layer-based task orchestrating method, NeutronOrch is memory-efficient. First, NeutronOrch saves the training memory requirement by offloading the computation to the CPU. Second, the cached objects of NeutronOrch are only historical embeddings for hot vertices within a super-batch, consuming only a small amount of GPU memory. Therefore, NeutronOrch can enable more GPU memory for accelerating sample and train steps while avoiding GPU memory contention.

(3) Comparison with GNNLab [49]: NeutronOrch achieves a speed-up ranging from $1.20\times$ (for GraphSAGE on Orkut) to $1.96\times$ (for GCN on Wiki) compared to GNNLab. NeutronOrch performs better when training with larger models or datasets. GNNLab needs to maintain the graph topology, cache data, and training data in the GPU memory, which constrains its scalability, especially when training billion-scale graphs like Papers100M for users with limited GPU resources. When the training memory requirement increases, GNNLab’s performance degrades due to a decrease in its cache hit rate. Moreover, when handling deeper GNN models, GNNLab encounters out-of-memory (OOM) issues due to GPU memory exhaustion, as shown in Table 6, Table 7, and Section 5.7.

(4) Comparison with DGL-UVA [42]: NeutronOrch achieves a speed-up ranging from $1.44\times$ (for GCN on Orkut) to $3.67\times$ (for GCN on PR) compared to DGL-UVA. DGL-UVA supports accessing graph topology and features via the zero-copy transfer engine [30]. We categorize DGL-UVA’s gather step on the CPU since it keeps all the features in the CPU memory with any feature caching. The zero-copy transfer engine helps the GPU accelerate the sampling step without saving the graph topology in GPU memory and eliminates the feature collection processing in the gathering step. Compared to saving the graph topology in the GPU for sampling, DGL-UVA saves GPU memory while introducing access latency between CPU and GPU. On the other hand, as discussed in Section 3, performing entire sample and train steps on the GPU can result in resource contention and prolonged execution time. Therefore, DGL-UVA has a larger communication compared to NeutronOrch because it transfers all features needed for training in every iteration.

(5) Comparison with GAS [10]: NeutronOrch achieves a speed-up ranging from $2.36\times$ (for GAT on Reddit) to $4.91\times$ (for GAT on PR) compared to GAS. This is because GAS computes historical

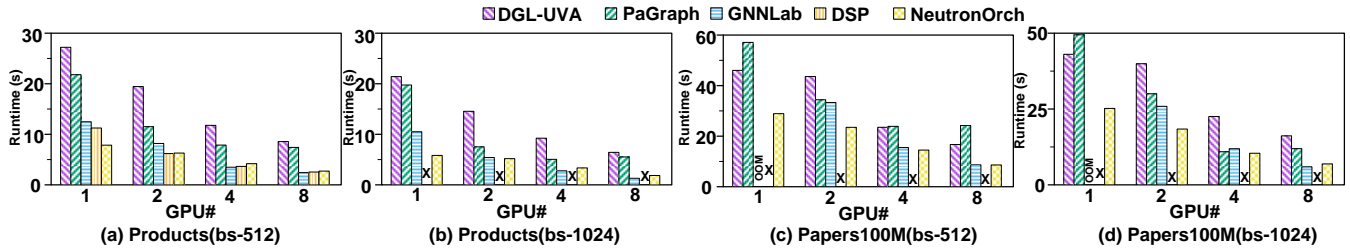


Figure 12: Per-epoch runtime of NeutronOrch and other systems under multi-GPU environment. (bs denotes batch size, “x” denotes illegal memory access, and “OOM” denotes out of memory).

embeddings for all vertices and transfers them back to the CPU memory. Although GPU memory is saved, additional overhead is incurred due to frequent CPU-GPU communication. GAS also faces CPU memory limitations on graphs with a large number of vertices, as it needs to store historical embeddings for all vertices across every layer. In contrast, NeutronOrch selectively computes historical embeddings for frequently accessed vertices on the CPU, achieving efficient historical embedding reuse while reducing memory overhead. Furthermore, NeutronOrch achieves higher accuracy with strictly bounded staleness than GAS, which arbitrarily reuses historical embeddings within an epoch (see more details in Section 5.8).

5.3 Multi-GPU Performance

Overall comparison. We conduct a comparative analysis of NeutronOrch, PaGraph [25], DGL-UVA [30], GNNLab [49], and DSP [4] to evaluate the scalability by varying the number of GPUs used in training. Figure 12 shows the results of training GraphSAGE against two real-world datasets with different numbers of GPUs. Compared to DGL-UVA [30] and PaGraph [25], NeutronOrch consistently demonstrates superior performance with different batch sizes and different numbers of GPUs. NeutronOrch achieves on average 2.53 \times and 2.19 \times speedups over DGL-UVA and PaGraph. The performance of DGL-UVA and PaGraph is limited by extensive CPU-GPU communication and inefficient CPU sampling. In contrast, NeutronOrch minimizes CPU-GPU communication by reusing the historical embeddings and adaptively adjusting the workload between CPU and GPUs. Compared to GNNLab [49] and DSP [4], NeutronOrch does not consistently demonstrate superior performance. On Products with 4 and 8 GPUs, DSP and GNNLab show better performance because their cache design effectively reduces CPU-GPU communication. However, when handling large-scale graphs (Papers100M), both DSP and GNNLab report memory errors due to memory exhaustion. Notably, DSP even fails to operate on small graphs when using a batch size of 1024. NeutronOrch effectively trains large-scale GNNs by offloading computations to the CPU, reducing both CPU-GPU communication and GPU memory overhead.

Scaling Performance. The execution time for all systems decreases as more GPUs are added. Specifically, when the number of GPUs increases from 1 to 8, the runtimes of NeutronOrch, PaGraph, DGL-UVA, GNNLab, and DSP decrease by 3.65 \times , 3.01 \times , 2.97 \times , 6.61 \times , and 5.86 \times , respectively. NeutronOrch, PaGraph, and DGL-UVA fail to achieve a speedup greater than 4 \times due to their reliance on CPU-GPU communication for data transfer. In our GPU server, the 8 GPUs are connected to the CPU through 4 PCIe switches, with each two GPUs sharing the same PCIe link to fetch data from the

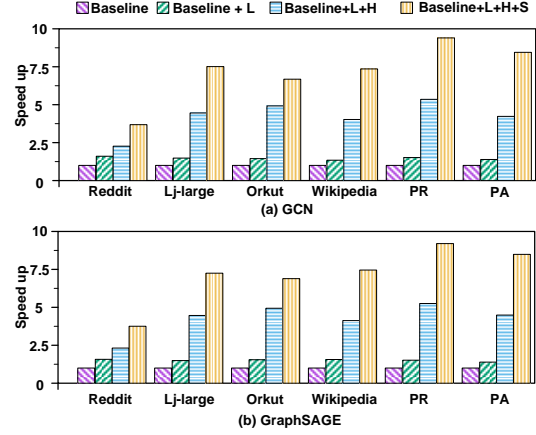


Figure 13: Performance gain analysis. L for the layer-based task orchestrating, H for the hotness-aware embedding reusing, and S for the super-batch pipelined training.

CPU, causing bandwidth contention during training. Among these three systems, NeutronOrch achieves better scaling performance by reducing CPU-GPU communication through historical embedding reuse. GNNLab and DSP achieve nearly linear speedup in successful runs. Nevertheless, their design, which involves caching vertex features and the entire graph topology, limits their ability to handle large-scale graphs. NeutronOrch consistently exhibits high efficiency in all scenarios thanks to the memory-efficient task orchestrating method.

5.4 Performance Gain Analysis

In this section, we analyze the performance gain of layer-based task orchestrating (L), hotness-aware embedding reusing (H), and super-batch pipelined training (S) on the GCN and GraphSAGE model with six datasets. We start from a baseline with NeutronOrch’s codebase for a fair comparison and gradually integrate three optimizations. The baseline is a step-based task orchestrating method that employs GPU-based graph sampling, GPU-based training, and CPU-based gather step. Figure 13 shows the normalized speedups. The baseline+L configuration aggregates and updates all vertex features on the CPU and transfers the vertex embedding to the GPU for computation, significantly reducing the CPU-GPU communication. It can achieve an average speedup of 1.52 \times compared to the baseline. The hotness-aware embedding reusing optimizes the layer-based task orchestrating of NeutronOrch, significantly reducing CPU computation. It provides an additional average speedup of 1.96 \times over the baseline+L. Finally, the super-batch pipeline design provides an additional average speedup of 1.65 \times over the baseline with L and

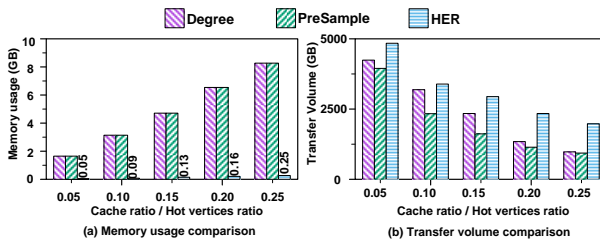


Figure 14: The memory usage and transfer volume comparison among different caching policies with hot vertices embedding reusing method.

H. This design enables the overlap of computations between the CPU and GPU, reducing overall execution time substantially.

5.5 Benefit of Hotness-Aware Layer-Based Task Orchestrating

We next explore how the hotness-aware layer-based task orchestrating method impacts the CPU-GPU communication, GPU memory consumption, and GPU computation.

We implement the degree-based cache policy (Degree) [25] and the pre-sampling-based cache policy (PreSample) [49] in NeutronOrch and compare them with hotness-aware embedding reusing method (HER). GNNLab and PaGraph propose reserving a portion of GPU memory for static caching of frequently accessed vertex features. In contrast, NeutronOrch offloads the bottom layer training of these vertices to the CPU and pulls vertex embeddings on-demand on the GPU side. Thanks to the hotness-aware embedding reusing method (HER) with bounded staleness, NeutronOrch achieves reduced transfer volume and saves GPU memory. Each hot vertex embedding in the CPU pulled by the GPU will save the transfer volume of its neighboring features, and hot vertex embedding in the GPU cache hit will save more transfer volume. Meanwhile, as designed in Section 4.3.1, in the GPU, NeutronOrch only needs to maintain the space needed for a hot vertices queue of one super-batch. This greatly saves GPU memory compared to traditional static caching policies and provides fine-grained historical embeddings for each super-batch.

To illustrate it, we conduct experiments using the GCN model on the Wikipedia dataset. Figure 14 (a) illustrates that the dynamic caching of historical embeddings in NeutronOrch leads to an average reduction of 98% in GPU memory usage compared to static cache policies like Degree and PreSample for different cache ratios and hot vertex ratios. Unlike static caching policies that require substantial GPU memory, NeutronOrch utilizes the available computational power of CPUs and minimal GPU memory to achieve comparable reductions in transfer volume. Under different cache ratios and hot vertices ratios, the average transfer volume using the HER method is 1.44 \times and 1.73 \times of the static caching strategies Degree and PreSample, respectively.

On the other hand, the computation volume of bottom-layer training in the GPU is significantly reduced since the CPU-provided hot vertex embeddings can be reused multiple times within the super-batch. A larger hot vertices ratio facilitates more GPU computation savings. The proportion of hot vertices is proportional to the CPU’s computing power. In order to guarantee the bound, the CPU must complete the hot vertices embeddings update of the next

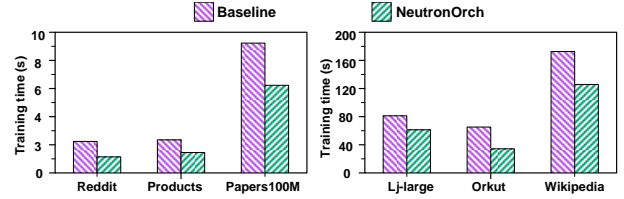


Figure 15: Average GPU training time in one epoch of Baseline and NeutronOrch.

Table 6: Per-epoch runtime of different systems with different model depth (GCN).

Systems	Products			Wiki		
	3-layer	4-layer	5-layer	3-layer	4-layer	5-layer
DGL	28.1	55.4	114.8	1669.1	OOM	OOM
PaGraph	20.1	45.0	78.0	1362.3	OOM	OOM
DGL-UVA	21.8	41.6	71.3	1209.2	2646.2	OOM
GNNLab	10.5	22.6	46.9	1152.4	OOM	OOM
GAS	26.2	30.9	35.2	OOM	OOM	OOM
NeutronOrch	5.82	11.9	20.9	590.3	1425.6	5940.8

Table 7: Per-epoch runtime of different systems with different batch sizes. (3-layer GCN)

Systems	Products				Wiki				
	Batch size		Batch size		Batch size		Batch size		
	256	1024	4096	10000		256	1024	4096	10000
DGL	35.1	28.1	11.9	5.24	2104.1	1669.1	861.9	OOM	OOM
PaGraph	31.6	20.1	15.5	11.9	1533.1	1362.3	OOM	OOM	OOM
DGL-UVA	30.1	21.8	8.87	4.99	1624.5	1209.2	592.4	301.6	301.6
GNNLab	16.5	10.5	5.42	3.31	1342.2	1152.4	OOM	OOM	OOM
GAS	56.4	26.2	18.1	15.1	OOM	OOM	OOM	OOM	OOM
NeutronOrch	9.51	5.82	2.92	1.79	846.2	590.3	265.2	185.4	185.4

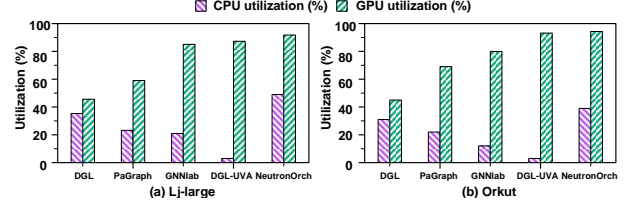


Figure 16: GPU utilization and CPU utilization comparison.

super-batch within one super-batch. The proportion of hot vertices that can be supported by different datasets is usually 10% -30%. We use the NeutronOrch with a hot vertices ratio of 0 as a baseline and compare the average GPU training time of one epoch with NeutronOrch. Figure 15 presents the observation of GPU training time reduction for GCN algorithms with six datasets. NeutronOrch reduced GPU training time by an average of 36.5% on six datasets. In addition, the reduction of GPU training time is most significant on Reddit and Orkut, with an average of 48.3%. This is because they have a larger average degree, which is great for improving hot vertices hits.

5.6 Analysis of Resource Utilization

We evaluate the utilization of GPU and CPU resources during the training of GCN on Lj-large and Orkut using five systems: DGL, PaGraph, GNNLab, DGL-UVA, and NeutronOrch. Figure 16 presents a comparison of GPU and CPU utilization. GPU and CPU utilization were recorded every 100 milliseconds and averaged over ten epochs. NeutronOrch exhibits superior utilization of both CPU and GPU resources by scheduling training tasks across CPUs and GPUs. DGL and PaGraph have good CPU utilization and poor GPU utilization. This is because performing a complete sampling or gathering step on the CPU improves CPU utilization but causes the GPU to wait. DGL-UVA and GNNLab have poor CPU utilization and good

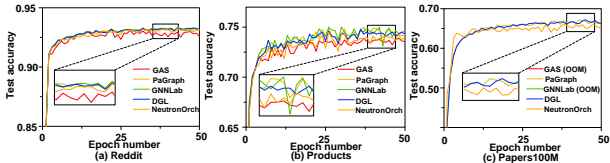


Figure 17: Epoch-to-accuracy on a 3-layer GCN

GPU utilization. They have good performance with sufficient GPU resources, but exploiting CPU resources can further improve performance. NeutronOrch achieves both good CPU and GPU utilization, averaging 44.5% and 92.9%, respectively.

5.7 Varying Model Configurations

Performance with varying model depths. As the model depth increases, the effectiveness of NeutronOrch will not decrease, although NeutronOrch only offloads the lowest-level calculations to the CPU. In sampling-based GNN training, the number of vertices exhibits exponential growth across layers [5, 14]. As a result, more than half of the entire training workload comes from the bottom layer. For example, on Wiki dataset with 3-layer model, the bottom layer has 1.94M vertices, occupying 65% of the total workload, while the other layers only have 1.04M vertices in total. For the 4-layer model and 5-layer model, the bottom layer occupies 61% and 59% of the total workload, respectively. We run a GCN model on all systems and report the per-epoch runtime in Table 6, with the model depth ranging from 3 to 5. For the 3-layer model, NeutronOrch achieves on average 2.97 \times speedup over the different systems. For the 4-layer model and 5-layer model, the speedups are 2.57 \times and 3.31 \times , respectively.

Performance with varying batch sizes. To study the effectiveness of NeutronOrch under different batch sizes, we run a 3-layer GCN model on all systems and report the per-epoch runtime in Table 7, with the batch size ranging from 256 to 10000. For a batch size of 256, NeutronOrch achieves on average 2.75 \times speedups over different systems. For batch sizes of 1024, 4096, and 10000, the speedups are 2.97 \times , 3.41 \times , and 3.07 \times , respectively. The setting of batch size will not affect the effectiveness. Furthermore, on large-scale graphs, NeutronOrch’s CPU offloading efficiently mitigates the increasing memory overhead when using large batch sizes.

5.8 Training Convergence

We plot the epoch-to-accuracy curve for different systems. Benefiting from the super-batch pipeline design, NeutronOrch can rigorously control the version difference of historical embeddings between two consecutive super-batches. As shown in Figure 17, compared to other GNN systems that use historical embeddings but do not strictly control versions (e.g., GAS [11]), NeutronOrch achieves higher accuracy. This is because NeutronOrch can achieve smaller cumulative errors across batches through version control. In comparison to systems that do not use historical embeddings, NeutronOrch achieves comparable convergence accuracy, with an accuracy loss of no more than 1%.

6 RELATED WORK

Full-batch GNN training. A set of GNN systems [3, 22, 26, 43, 54] adopt full-batch GNN training to guarantee high accuracy. NeuGraph [26] defines a new, flexible SAGA-NN model to express GNNs.

It fuses graph operations into TensorFlow and supports training on multiple GPUs. ROC [22] optimizes graph partitioning with online learning while managing memory with dynamic programming. For effective GNN training on several GPUs, DGCL [3] designs a communication planning algorithm that avoids conflict on various links. Neutronstar [43] designs hybrid dependency management for a more balanced use of communication and computational resources.

Sample-based mini-batch GNN training. GraphSage [14] first introduces the fixed-number vertex sampling and proposes the general message aggregation methods. Past works mainly focused on solving the sampling and gathering bottleneck in sample-based GNN training. For the sampling step, LazyGCN [37] proposes a sample graph reusing method to reduce sampling overhead and maintain accuracy. MariusGNN [41] design the DENSE data structure to minimize redundant computation in multi-hop sampling. On the other hand, Nextdoor [21], Wholegraph [47], and TurboGNN [45] propose the GPU-based sampling method to accelerate the sampling step. For the gathering step, a series of feature and graph caching strategies are proposed. Data tiering [29], and Quiver [39] design various efficient GPU feature cache strategies to minimize the CPU-GPU communication. Ducati [52] further designs the graph topology cache method to fully utilize the GPU memory.

Historical embeddings reusing. Existing works [6, 10, 17, 34] have shown the benefits of historical embedding (HE) reuse for training acceleration without compromising accuracy. VR-GCN [6] uses HE in GNN training to reduce the variance and further control the number of nodes to sample. Refresh [17] uses a combination of gradient-based and staleness criteria to reduce estimation errors. SANCUS [34] reuses HE for boundary vertices to reduce communication in distributed GNN training. These frameworks focus on optimizing scenarios where computation is exclusively deployed on GPUs. In contrast, our work extends HE reuse to the CPU-GPU environment, achieving both high performance and scalability.

Task orchestrating in DNN training. Zero-Infinity DeepSpeed (ZID) [28] incorporates CPU offload techniques [35, 36, 38] to optimize the DNN training under heterogeneous environments. Although ZID and our design share similarities in scheduling training tasks across CPU and GPUs to improve scalability, their optimization objectives are different. ZID primarily focuses on reducing the memory consumption of model parameters, reducing memory consumption by offloading model parameters to the CPU. In DNNs, model parameters which consist of dense matrices that can be disjointly partitioned. These slices can be efficiently communicated between the CPU and GPUs because of their dense and regular data access patterns. In contrast, NeutronOrch primarily focuses on the efficiency of sample-based GNN training, minimizing communication and computation by offloading historical embedding computation to the CPU. Sample-based GNN training involves multiple data preparation stages (sample and gather). It exhibits irregular vertex access patterns due to the inherent complexity of graph structures, which pose new challenges in optimizing the data I/O between CPU and GPUs. ZID didn’t address these challenges. However, NeutronOrch effectively resolves these problems by its task orchestrating method, transferring and reusing historical embedding for frequently accessed vertices.

7 CONCLUSION

We present NeutronOrch, a scalable and efficient GNN training system that fully utilizes CPU and GPUs. NeutronOrch leverages two key components to achieve its performance, including a hotness-aware layer-based task orchestrating method that combines CPU computation offloading with historical embeddings reuse to optimize computation and communication and a super-batch pipeline training method that utilizes CPU-GPU pipelining to achieve efficient and staleness-bounded version control. Our experiments demonstrate that NeutronOrch efficiently accelerates mini-batch GNN training with an accuracy loss of no more than 1%.

REFERENCES

[1] Lars Backstrom, Daniel P. Huttenlocher, Jon M. Kleinberg, and Xiangyang Lan. 2006. Group formation in large social networks: membership, growth, and evolution. In *Proceedings of the Twelfth ACM SIGKDD International Conference on Knowledge Discovery and Data Mining, KDD'06, Philadelphia, PA, USA*, 44–54.

[2] Jasmijn Bastings, Ivan Titov, Wilker Aziz, Diego Marcheggiani, and Khalil Sima'an. 2017. Graph Convolutional Encoders for Syntax-aware Neural Machine Translation. In *Proceedings of the 2017 Conference on Empirical Methods in Natural Language Processing, EMNLP'17, Copenhagen, Denmark*. Association for Computational Linguistics, 1957–1967.

[3] Zhenkun Cai, Xiao Yan, Yidi Wu, Kaihao Ma, James Cheng, and Fan Yu. 2021. DGCL: an efficient communication library for distributed GNN training. In *Sixteenth European Conference on Computer Systems, EuroSys '21, Online Event, United Kingdom*. ACM, 130–144.

[4] Zhenkun Cai, Qihui Zhou, Xiao Yan, Da Zheng, Xiang Song, Chenguang Zheng, James Cheng, and George Karypis. 2023. DSP: Efficient GNN Training with Multiple GPUs. In *Proceedings of the 28th ACM SIGPLAN Annual Symposium on Principles and Practice of Parallel Programming, PPoPP'23, Montreal, QC, Canada*. ACM, 392–404.

[5] Jie Chen, Tengfei Ma, and Cao Xiao. 2018. FastGCN: Fast Learning with Graph Convolutional Networks via Importance Sampling. In *6th International Conference on Learning Representations, ICLR'18, Vancouver, BC, Canada*. OpenReview.net.

[6] Jianfei Chen, Jun Zhu, and Le Song. 2018. Stochastic Training of Graph Convolutional Networks with Variance Reduction. In *Proceedings of the 35th International Conference on Machine Learning, ICML'18, Stockholm, Sweden (Proceedings of Machine Learning Research, Vol. 80)*. PMLR, 941–949.

[7] Ahmed El-Kishky, Michael M. Bronstein, Ying Xiao, and Aria Haghighi. 2022. Graph-based Representation Learning for Web-scale Recommender Systems. In *The 28th ACM SIGKDD Conference on Knowledge Discovery and Data Mining, KDD'22, Washington, DC, USA*, Aidong Zhang and Huzeifa Rangwala (Eds.). ACM, 4784–4785.

[8] Wenqi Fan, Yao Ma, Qing Li, Yuan He, Yihong Eric Zhao, Jiliang Tang, and Dawei Yin. 2019. Graph Neural Networks for Social Recommendation. In *The World Wide Web Conference, WWW'19, San Francisco, CA, USA*. ACM, 417–426.

[9] Matthias Fey and Jan Eric Lenssen. 2019. Fast Graph Representation Learning with PyTorch Geometric. *CoRR* abs/1903.02428 (2019).

[10] Matthias Fey, Jan Eric Lenssen, Frank Weichert, and Jure Leskovec. 2021. GNAutoScale: Scalable and Expressive Graph Neural Networks via Historical Embeddings. In *Proceedings of the 38th International Conference on Machine Learning, ICML 2021, 18–24 July 2021, Virtual Event (Proceedings of Machine Learning Research, Vol. 139)*. Marina Meila and Tong Zhang (Eds.). PMLR, 3294–3304.

[11] Swapnil Gandhi and Anand Padmanabha Iyer. 2021. P3: Distributed Deep Graph Learning at Scale. In *15th USENIX Symposium on Operating Systems Design and Implementation, OSDI'21*. USENIX Association, 551–568.

[12] Zhangxiaowen Gong, Houxiang Ji, Yao Yao, Christopher W. Fletcher, Christopher J. Hughes, and Josep Torrellas. 2022. Graphite: optimizing graph neural networks on CPUs through cooperative software-hardware techniques. In *The 49th Annual International Symposium on Computer Architecture, ISCA'22, New York, USA*. ACM, 916–931.

[13] William L. Hamilton, Rex Ying, and Jure Leskovec. 2017. Representation Learning on Graphs: Methods and Applications. *IEEE Data Eng. Bull.* 40, 3 (2017), 52–74.

[14] William L. Hamilton, Zhitao Ying, and Jure Leskovec. 2017. Inductive Representation Learning on Large Graphs. In *Advances in Neural Information Processing Systems 30: Annual Conference on Neural Information Processing Systems 2017, NeurIPS'17 Long Beach, CA, USA*. 1024–1034.

[15] Qirong Ho, James Cipar, Henggang Cui, Seunghak Lee, Jin Kyu Kim, Phillip B. Gibbons, Garth A. Gibson, Gregory R. Ganger, and Eric P. Xing. 2013. More Effective Distributed ML via a Stale Synchronous Parallel Parameter Server. In *Advances in Neural Information Processing Systems 26: 27th Annual Conference on Neural Information Processing Systems 2013, NeurIPS'12, Lake Tahoe, Nevada, United States*. 1223–1231.

[16] Weihua Hu, Matthias Fey, Marinka Zitnik, Yuxiao Dong, Hongyu Ren, Bowen Liu, Michele Catasta, and Jure Leskovec. 2020. Open Graph Benchmark: Datasets for Machine Learning on Graphs. In *Advances in Neural Information Processing Systems 33: Annual Conference on Neural Information Processing Systems 2020, NeurIPS'20, December 6–12*.

[17] Kezhoa Huang, Haitian Jiang, Minjie Wang, Guangxuan Xiao, David Wipf, Xiang Song, Quan Gan, Zengfeng Huang, Jidong Zhai, and Zheng Zhang. 2023. ReFresh: Reducing Memory Access from Exploiting Stable Historical Embeddings for Graph Neural Network Training. *CoRR* abs/2301.07482 (2023).

[18] Kezhoa Huang, Jidong Zhai, Zhen Zheng, Youngmin Yi, and Xipeng Shen. 2021. Understanding and bridging the gaps in current GNN performance optimizations. In *26th ACM SIGPLAN Symposium on Principles and Practice of Parallel Programming, PPoPP '21, Virtual Event, Republic of Korea*. ACM, 119–132.

[19] Kezhoa Huang, Jidong Zhai, Zhen Zheng, Youngmin Yi, and Xipeng Shen. 2021. Understanding and bridging the gaps in current GNN performance optimizations. In *26th ACM SIGPLAN Symposium on Principles and Practice of Parallel Programming, Virtual Event, PPoPP '21, Republic of Korea*. ACM, 119–132.

[20] Ihab F. Ilyas, Theodoros Rekatsinas, Vishnu Konda, Jeffrey Pound, Xiaoguang Qi, and Mohamed A. Soliman. 2022. Saga: A Platform for Continuous Construction and Serving of Knowledge at Scale. In *International Conference on Management of Data, SIGMOD'22, Philadelphia, PA, USA*. ACM, 2259–2272.

[21] Abhinav Jangda, Sandeep Polisetty, Arjun Guha, and Marco Serafini. 2021. Accelerating graph sampling for graph machine learning using GPUs. In *Sixteenth European Conference on Computer Systems, EuroSys '21, Online Event, United Kingdom*, Antonio Barbalace, Pramod Bhatotia, Lorenzo Alvisi, and Cristian Cadar (Eds.). ACM, 311–326.

[22] Zhihao Jia, Sina Lin, Mingyu Gao, Matei Zaharia, and Alex Aiken. 2020. Improving the Accuracy, Scalability, and Performance of Graph Neural Networks with Roc. In *Proceedings of Machine Learning and Systems 2020, MLSys'20, Austin, TX, USA*, Inderjit S. Dhillon, Dimitris S. Papailiopoulos, and Vivienne Sze (Eds.). mlsys.org.

[23] Thomas N. Kipf and Max Welling. 2017. Semi-Supervised Classification with Graph Convolutional Networks. In *5th International Conference on Learning Representations, ICLR'17, Toulon, France, Conference Track Proceedings*. OpenReview.net.

[24] Jérôme Kunegis. 2013. KONECT: the Koblenz network collection. In *22nd International World Wide Web Conference, WWW'13, Rio de Janeiro, Brazil*. International World Wide Web Conferences Steering Committee / ACM, 1343–1350.

[25] Zhiqi Lin, Cheng Li, Youshan Miao, Yunxin Liu, and Yinlong Xu. 2020. PaGraph: Scaling GNN training on large graphs via computation-aware caching. In *ACM Symposium on Cloud Computing, SoCC'20, Virtual Event, USA*. ACM, 401–415.

[26] Lingxiao Ma, Zhi Yang, Youshan Miao, Jilong Xue, Ming Wu, Lidong Zhou, and Yafei Dai. 2019. NeuGraph: Parallel Deep Neural Network Computation on Large Graphs. In *2019 USENIX Annual Technical Conference, ATC'19, Renton, WA, USA*. USENIX Association, 443–458.

[27] Steffen Maass, Changwoo Min, Sanidhya Kashyap, Woon-Hak Kang, Mohan Kumar, and Taesoon Kim. 2017. Mosaic: Processing a Trillion-Edge Graph on a Single Machine. In *Proceedings of the Twelfth European Conference on Computer Systems, EuroSys'17, Belgrade, Serbia*. ACM, 527–543.

[28] Microsoft. 2020. Extreme-scale model training for everyone. <https://www.microsoft.com/en-us/research/blog/deepspeed-extreme-scalemode-training-for-everyone>.

[29] Seungwon Min, Kun Wu, Mert Hidayetoglu, Jinjun Xiong, Xiang Song, and Wen-Mei Hwu. 2022. Graph Neural Network Training and Data Tiering. In *The 28th ACM SIGKDD Conference on Knowledge Discovery and Data Mining, KDD'22, Washington, DC, USA*. ACM, 3555–3565.

[30] Seungwon Min, Kun Wu, Saito Huang, Mert Hidayetoglu, Jinjun Xiong, Eiman Ebrahimi, Deming Chen, and Wen-mei W. Hwu. 2021. Large Graph Convolutional Network Training with GPU-Oriented Data Communication Architecture. *Proc. VLDB Endow.* 14, 11 (2021), 2087–2100.

[31] Jason Mohoney, Roger Waleffe, Henry Xu, Theodoros Rekatsinas, and Shivararam Venkataraman. 2021. Marius: Learning Massive Graph Embeddings on a Single Machine. In *15th USENIX Symposium on Operating Systems Design and Implementation, OSDI'21*. USENIX Association, 533–549.

[32] NVIDIA. 2022. DGX Systems. <https://www.nvidia.com/en-sg/data-center/dgx-systems/dgx-1>.

[33] Adam Paszke, Sam Gross, Francisco Massa, Adam Lerer, James Bradbury, Gregory Chanan, Trevor Killeen, Zeming Lin, Natalia Gimelshein, Luca Antiga, Alban Desmaison, Andrean Köpf, Edward Z. Yang, Zachary DeVito, Martin Raison, Alykhan Tejani, Sasank Chilamkurthy, Benoit Steiner, Lu Fang, Junjie Bai, and Soumith Chintala. 2019. PyTorch: An Imperative Style, High-Performance Deep Learning Library. In *Advances in Neural Information Processing Systems 32: Annual Conference on Neural Information Processing Systems 2019, NeurIPS'19, December 8–14, 2019, Hanna M. Wallach, Hugo Larochelle, Alina Beygelzimer, Florence d'Alché-Buc, Emily B. Fox, and Roman Garnett (Eds.)*. 8024–8035.

[34] Jingshu Peng, Zhao Chen, Yingxia Shao, Yanyan Shen, Lei Chen, and Jiannong Cao. 2022. SANCUS: Staleness-Aware Communication-Avoiding Full-Graph

Decentralized Training in Large-Scale Graph Neural Networks. *Proc. VLDB Endow.* 15, 9 (2022), 1937–1950.

[35] Samyam Rajbhandari, Jeff Rasley, Olatunji Ruwase, and Yuxiong He. 2020. ZeRO: memory optimizations toward training trillion parameter models. In *Proceedings of the International Conference for High Performance Computing, Networking, Storage and Analysis, SC’20, Virtual Event / Atlanta, Georgia, USA*. IEEE/ACM, 20.

[36] Samyam Rajbhandari, Olatunji Ruwase, Jeff Rasley, Shaden Smith, and Yuxiong He. 2021. ZeRO-infinity: breaking the GPU memory wall for extreme scale deep learning. In *International Conference for High Performance Computing, Networking, Storage and Analysis, SC’21, St. Louis, Missouri, USA*. ACM, 59.

[37] Morteza Ramezani, Weilin Cong, Mehrdad Mahdavi, Anand Sivasubramaniam, and Mahmut T. Kandemir. 2020. GCN meets GPU: Decoupling “When to Sample” from “How to Sample”. In *Advances in Neural Information Processing Systems 33: Annual Conference on Neural Information Processing Systems 2020, NeurIPS’20, virtual, Hugo Larochelle, Marc’Aurelio Ranzato, Raia Hadsell, Maria-Florina Balcan, and Hsuan-Tien Lin (Eds.)*.

[38] Jie Ren, Samyam Rajbhandari, Reza Yazdani Aminabadi, Olatunji Ruwase, Shuangyan Yang, Minjia Zhang, Dong Li, and Yuxiong He. 2021. ZeRO-Offload: Democratizing Billion-Scale Model Training. In *2021 USENIX Annual Technical Conference, ATC’21, USENIX Association*, 551–564.

[39] Zeyuan Tan, Xiulong Yuan, Congjie He, Man-Kit Sit, Guo Li, Xiaoze Liu, Baole Ai, Kai Zeng, Peter R. Pietzuch, and Luo Mai. 2023. Quiver: Supporting GPUs for Low-Latency, High-Throughput GNN Serving with Workload Awareness. *CoRR* abs/2305.10863 (2023).

[40] Petar Veličković, Guillem Cucurull, Arantxa Casanova, Adriana Romero, Pietro Liò, and Yoshua Bengio. 2018. Graph Attention Networks. In *6th International Conference on Learning Representations, ICLR’18, Vancouver, BC, Canada, Conference Track Proceedings*. OpenReview.net.

[41] Roger Waleffe, Jason Mohoney, Theodoros Rekatsinas, and Shivararam Venkataraman. 2022. Marius++: Large-Scale Training of Graph Neural Networks on a Single Machine. *CoRR* abs/2202.02365 (2022).

[42] Minjie Wang, Lingfan Yu, Da Zheng, Quan Gan, Yu Gai, Zihao Ye, Mufei Li, Jinjing Zhou, Qi Huang, Chao Ma, Ziyue Huang, Qipeng Guo, Hao Zhang, Haibin Lin, Junbo Zhao, Jinyang Li, Alexander J. Smola, and Zheng Zhang. 2019. Deep Graph Library: Towards Efficient and Scalable Deep Learning on Graphs. *CoRR* abs/1909.01315 (2019).

[43] Qiang Wang, Yanfeng Zhang, Hao Wang, Chaoyi Chen, Xiaodong Zhang, and Ge Yu. 2022. NeutronStar: Distributed GNN Training with Hybrid Dependency Management. In *International Conference on Management of Data, Philadelphia, SIGMOD’22, PA, USA*, Zachary Ives, Angela Bonifati, and Amr El Abbadi (Eds.). ACM, 1301–1315.

[44] Wei Wu, Bin Li, Chuan Luo, and Wolfgang Nejdl. 2021. Hashing-Accelerated Graph Neural Networks for Link Prediction. In *The Web Conference 2021, WWW’21, Virtual Event / Ljubljana, Slovenia*. ACM / IW3C2, 2910–2920.

[45] Wenchao Wu, Xuanhua Shi, Ligang He, and Hai Jin. 2023. TurboGNN: Improving the End-to-End Performance for Sampling-Based GNN Training on GPUs. *IEEE Trans. Comput.* (2023).

[46] Zonghan Wu, Shirui Pan, Fengwen Chen, Guodong Long, Chengqi Zhang, and Philip S. Yu. 2021. A Comprehensive Survey on Graph Neural Networks. *IEEE Trans. Neural Networks Learn. Syst.* 32, 1 (2021), 4–24.

[47] Dongxu Yang, Junhong Liu, Jiaxing Qi, and Junjie Lai. 2022. WholeGraph: A Fast Graph Neural Network Training Framework with Multi-GPU Distributed Shared Memory Architecture. In *International Conference for High Performance Computing, Networking, Storage and Analysis, SC’22, Dallas, TX, USA*. IEEE, 1–14.

[48] Jaewon Yang and Jure Leskovec. 2015. Defining and evaluating network communities based on ground-truth. *Knowl. Inf. Syst.* 42, 1 (2015), 181–213.

[49] Jianbang Yang, Dahai Tang, Xiaoniu Song, Lei Wang, Qiang Yin, Rong Chen, Wenyuan Yu, and Jingren Zhou. 2022. GNNLab: a factored system for sample-based GNN training over GPUs. In *Seventeenth European Conference on Computer Systems, EuroSys ’22, Rennes, France*. ACM, 417–434.

[50] Rex Ying, Ruining He, Kaifeng Chen, Pong Eksombatchai, William L. Hamilton, and Jure Leskovec. 2018. Graph Convolutional Neural Networks for Web-Scale Recommender Systems. In *Proceedings of the 24th ACM SIGKDD International Conference on Knowledge Discovery & Data Mining, KDD’18, London, UK*. ACM, 974–983.

[51] Muhan Zhang and Yixin Chen. 2018. Link Prediction Based on Graph Neural Networks. In *Advances in Neural Information Processing Systems 31: Annual Conference on Neural Information Processing Systems 2018, NeurIPS’18, Montréal, Canada*. 5171–5181.

[52] Xin Zhang, Yanyan Shen, Yingxia Shao, and Lei Chen. 2023. DUCATI: A Dual-Cache Training System for Graph Neural Networks on Giant Graphs with the GPU. *Proc. ACM Manag. Data* 1, 2 (2023), 166:1–166:24.

[53] Ziwei Zhang, Peng Cui, and Wenwu Zhu. 2022. Deep Learning on Graphs: A Survey. *IEEE Trans. Knowl. Data Eng.* 34, 1 (2022), 249–270.

[54] Da Zheng, Chao Ma, Minjie Wang, Jinjing Zhou, Qidong Su, Xiang Song, Quan Gan, Zheng Zhang, and George Karypis. 2020. DistDGL: Distributed Graph Neural Network Training for Billion-Scale Graphs. In *10th IEEE/ACM Workshop on Irregular Applications: Architectures and Algorithms, IA3’20, Atlanta, GA, USA*. IEEE, 36–44.

[55] Jie Zhou, Ganqu Cui, Shengding Hu, Zhengyan Zhang, Cheng Yang, Zhiyuan Liu, Lifeng Wang, Changcheng Li, and Maosong Sun. 2020. Graph neural networks: A review of methods and applications. *AI Open* 1 (2020), 57–81.